

Airline Planning Benchmark Problems

Part I: Characterising Networks and Demand using Limited Data

Kerem Akartunali^a, Natashia Boland^b, Ian Evans^c, Mark Wallace^d, Hamish Waterer^{b,d,*}

^aDepartment of Mathematics and Statistics, University of Melbourne, Parkville VIC 3010, Australia

^bSchool of Mathematical and Physical Sciences, University of Newcastle, Callaghan NSW 2308, Australia

^cConstraint Technologies International, Level 7 224 Queen St, Melbourne VIC 3000, Australia

^dFaculty of Information Technology, Monash University, Caulfield VIC 3145, Australia

Abstract

This paper is the first of two papers entitled “Airline Planning Benchmark Problems”, aimed at developing benchmark data that can be used to stimulate innovation in airline planning, in particular, in flight schedule design and fleet assignment. While optimisation has made an enormous contribution to airline planning in general, the area suffers from a lack of standardised data and benchmark problems. Current research typically tackles problems unique to a given carrier, with associated specification and data unavailable to the broader research community. This limits direct comparison of alternative approaches, and creates barriers of entry for the research community. Furthermore, flight schedule design has, to date, been under-represented in the optimisation literature, due in part to the difficulty of obtaining data that adequately reflects passenger choice, and hence schedule revenue. This is Part I of two papers taking first steps to address these issues. It does so by providing a framework and methodology for generating realistic airline demand data, controlled by scalable parameters. First, a characterisation of flight network topologies and network capacity distributions is deduced, based on analysis of airline data. Then a bi-objective optimisation model is proposed to solve the inverse problem of inferring OD-pair demands from passenger loads on arcs. These two elements are combined to yield a methodology for generating realistic flight network topologies and OD-pair demand data, according to specified parameters. This methodology is used to produce 33 benchmark instances exhibiting a range of characteristics. Part II will extend this work by partitioning the demand in each market (OD pair) into market segments, each with its own utility function and set of preferences for alternative airline products. The resulting demand data will better reflect recent empirical research on passenger preference, and is expected to facilitate passenger choice modelling in flight schedule optimisation.

Keywords: Airline planning, benchmark data, inverse problems

1. Introduction

This paper is the first of two papers entitled “Airline Planning Benchmark Problems”. The primary goal in these papers is to stimulate and facilitate further research in airline planning. There has been relatively little work that has addressed the first stage of the airline planning process, namely, flight schedule design. The many algorithms and techniques reported in the literature for latter stages of the airline planning process are difficult to compare because they are evaluated on problem instances representative of a particular airline at a particular date. Each airline operates a different network of airports, a different fleet in terms of the size and mix of aircraft, has different passenger quantities and itineraries, and different crew requirements, bases and rules. Furthermore, the data for these instances is considered confidential by most airlines due to its significant

commercial implications. Consequently, obtaining real data is difficult and often requires the researcher to establish a good relationship with an airline partner over many years. Such issues create a barrier to entry for many prospective researchers and limits potentially fruitful collaboration between research groups.

Some first steps towards addressing these issues are taken in these two papers by developing a framework for generating realistic benchmark instances. These instances provide standardised data with which to initiate the airline planning process. Since flight schedule design depends critically on market demand, this initial work has focussed on the generation of airline demand benchmark data. The addition of airline resources, such as aircraft and crew, to these benchmarks is planned for the future. By making these instances, and a description of the methodology used to generate them, publicly available it is hoped that research engagement in airline planning will be stimulated in a similar way to what has been so successfully achieved in areas such as vehicle routing, which flourished after the introduction of the Solomon benchmark instances (Solomon,

*Corresponding author

Email addresses: k.akartunali@ms.unimelb.edu.au (Kerem Akartunali), natashia.boland@newcastle.edu.au (Natashia Boland), ian.evans@contecint.com.au (Ian Evans), mark.wallace@infotech.monash.edu.au (Mark Wallace), hamish.waterer@newcastle.edu.au (Hamish Waterer)

1987). The DIMACS¹ and ROADEF² challenge instances have had a similar impact.

As a large body of literature attests, optimisation has been a critical part of airline planning for many decades. See, for example, Klabjan (2005) or Bazargan (2004). However, as noted in Klabjan (2005), for the most part, airline schedule planning is a manual process with only a few manuscripts on flight schedule design. Notable among these are two papers, Yan and Tseng (2002) and Yan, Tang, and Lee (2007), on flight scheduling in Taiwan, and that of Lohatepanont and Barnhart (2004), combining flight scheduling with fleet assignment. The authors of this paper believe that the dearth of optimisation research on schedule design is in part due to the difficulty of representing passenger choice, and of collecting adequate data to accurately assess schedule revenue. However, there has been a growing body of both empirical and theoretical research seeking to provide insight into airline passenger decision processes and to develop models of passenger utility. See, for example, Coldren, Koppelman, Kasturirangan, and Mukherjee (2003), Garrow, Jones, and Parker (2007), Koppelman, Coldren, and Parker (2008), Walker (2006), and Wojahn (2002). The insights provided in these papers, combined with an empirical analysis of rich data sets from a wide range of airlines worldwide, including all airlines in the Star and oneworld alliances, has led to the development of a new approach to representing airline demand data, and a methodology for generating realistic demand data sets.

The methodology developed in these two papers is a four step framework. Figure 1 illustrates the four steps in the framework which are:

1. Generate the flight network including passenger load on arcs;
2. Calculate origin-destination (OD) pair demand;
3. Define passenger groups;
4. Allocate OD-pair demand to each passenger group.

The flight network connects the set of airports to be served, and the network topology defines arcs indicating airport pairs between which direct non-stop services are to be offered. Passenger load on an arc indicates the total number of passengers expected to travel on the direct non-stop service over some time period, for example, a day.

This paper presents the methodology behind the first two steps in this framework. The first step generates realistic flight networks and passenger loads with specified characteristics that capture the features of a large fraction of existing airline networks. These networks are scalable so that the effect of different scheduling strategies, and different parameters such as network type and size, or fleet mix, on algorithm performance and solution cost can be readily compared. The second step of the framework solves an inverse problem to determine OD-pair based demand that is compatible with the passenger loads on each arc. This data, sometimes called *market demand*, can

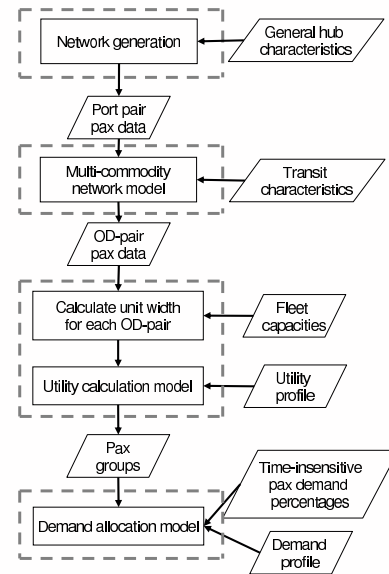


Figure 1: Framework for generating sets of realistic airline planning benchmark problem instances

be of use in its own right. For example, in performing schedule design, Yan and Tseng (2002) work directly from such data collected from airlines in Taiwan.

The second paper (Akartunali, Boland, Evans, Wallace, and Waterer, 2010a) presents the methodology behind the third and fourth steps in this framework. The third step partitions the market demand into *passenger groups*, according to characteristics that differentiate behaviour in terms of airline product selection. Each passenger group has an origin, a destination, a size (number of passengers), a departure time window, and a departure time utility curve indicating the passengers' willingness to pay for departure in time sub-windows. This data is much richer than simple market demand and can be expected to provide better estimates of schedule revenue in a form that is useful in schedule design optimisation. The integrated airline schedule design and fleet assignment problem studied in a companion paper (Akartunali, Boland, Evans, Wallace, Waterer, and Smith, 2010b) demonstrates passenger groups to be a potential alternative to the commonly used spill models (Dumas and Soumis, 2008; Jacobs, Smith, and Johnson, 2008; Barnhart, Farahat, and Lohatepanont, 2009) for estimating passenger flow in an airline network. The fourth step in the framework allocates the previously determined OD-pair demand to each passenger group using a standardised *demand profile*, a generic percentage-wise allocation of passengers throughout a day.

The design of this methodology readily permits the generation of realistic airline data "from scratch" in a way that supports experimentation with key characteristics of that data, as well as providing an approach that other researchers can still use when they have access to partial data. For example, if an existing flight network is already known, and, perhaps, observed passenger loads are also known for that network.

¹<http://dimacs.rutgers.edu/Challenges/>

²<http://challenge.roadef.org/>

1.1. Terminology, notation, and assumptions

An airline network consists of a set S of *ports* to be served, and a set $A \subseteq S \times S$ of directed *arcs* indicating an ordered pair of ports between which at least one direct non-stop service is offered. An airline's *fleet* is denoted by the set F of aircraft subtypes, and an aircraft from the fleet $f \in F$ has capacity c_f . The basic time unit used is one day. Let \mathcal{T} denote the length of a day in minutes.

Let $\bar{K} \subset S \times S$ denote the set of ordered potential passenger *origin-destination pairs*, or OD-pairs. For each OD-pair $(o, d) \in \bar{K}$, the *OD-pair demand* D_{od} is the total passenger demand over a day to travel from port o to port d . In the case that an OD-pair is not an arc then the only way passengers can complete their travel is to connect to successive arcs by *transiting* at an intermediate port. The passenger load n_{ij} on arc $(i, j) \in A$ is the number of passengers observed traversing the arc over the course of a day.

1.2. Overview of the paper

Section 2 describes methodology to characterise airline networks. This is the first step in the framework for generating sets of realistic airline planning benchmark problems. Section 3 describes methodology to characterise airline demand using limited data. This is the second step in the framework. A description of the generated benchmark instances is provided in Section 4 and an analysis of the instances is given in Section 5. Section 6 presents some conclusions and a brief description of future work.

2. Characterising airline networks

An airline network's topology depends on factors such as the geographical positions of the ports serviced by the network, the desired operating practices of the airline, the structure of the network of any competitors, and also passenger demand. This paper concentrates on the commonly occurring *hub-and-spoke* topology. This topology consists of a single *hub* airport connected by flight legs to a number of *spoke* airports. The spoke airports are only connected to the hub, that is, no flight legs exist between spoke airports.

Evans, Wallace, and Waterer (2010) analysed data from a wide range of airlines worldwide, including all airlines from Star and oneworld alliances, and found that more than 80% of airports are connected in topologies that resemble hub-and-spoke networks. Thus, analysing such networks is a critical first step. Moreover, more complex topologies such as those consisting of linked hubs, or point-to-point networks, require significantly more analysis.

2.1. Hub-and-spoke networks

The characteristics of hub-and-spoke networks were analysed by Evans et al. (2010) using data collected from the schedules operating at the end of 2007 and early 2008 for a wide range of airlines worldwide, including all airlines in the Star and oneworld alliances. Legs included in the analysis were restricted to those operated by common turbo-fan aircraft. The

aircraft capacity on each leg was used as a surrogate for passenger load due to the lack of actual passenger data. This section provides an overview of this characterisation.

Of the 64 hub-and-spoke networks included in the analysis, 41 were classified as short-haul networks as there were no arcs with a great-circle distance greater than 5000km, 10 were classified as long-haul as there existed arcs with a great-circle distance greater than 9500km, and the remaining 13 networks were classified as medium-haul. The statistical analysis of these networks focussed on characterising three distributions. The first was the greater-circle length of the network arcs, or the *arc distance*. The second characteristic was the capacities of the aircraft operating within the network, or the *arc capacity*. Finally, the third characteristic was the radial direction of the arcs and their associated capacity, or the *directional capacity*.

The analysis found that the distributions of arc distance for most networks could be clustered into five groups. Each distribution in a particular group was found to be statistically most similar to the other distributions in that group. Two of these groups corresponded to short-haul networks, two to long-haul, and the remaining group to medium-haul. A simple analytical model of an arc distance cumulative distribution function (CDF) was constructed for each group. The CDF was constructed so that it was a good fit to all of the arc distance distributions in that group.

Using a similar analysis, the distributions of arc capacity for most networks could also be clustered into five groups. Similarly, a simple analytical model of an arc capacity CDF was constructed for each group. An analysis of the correlation between arc distance and arc capacity CDFs showed that each arc distance CDF was strongly correlated to one of only two arc capacity CDFs. Short- and medium-haul networks shared the same arc capacity CDF while long-haul networks shared another arc capacity CDF.

To analyse the directional capacity of each network the arcs were partitioned into radial 15-degree sectors. The first sector included spokes radiating from the hub at angles $[0^\circ, 15^\circ)$, where angles were measured anticlockwise from due east, with the remaining sectors continuing in an anticlockwise direction. The capacity of a sector is given by the sum of the capacities of the network arcs in that sector.

The analysis found that there is often a major axis along which most capacity is concentrated, and this is most often closer to an East-West orientation than a North-South orientation. The position of the *greater lobe* of the major axis was defined to be the angle central to the four contiguous sectors with maximum total arc capacity. The position of the *lesser lobe* of the major axis was defined to be the angle central to the four contiguous sectors with maximum total arc capacity subject to the angle being at least 90° from the angle of the greater lobe. These lobes can range from being close to symmetrical to being extremely asymmetrical, that is, in some cases almost all capacity occurs in a lobe towards a single direction from the hub, with only a small amount of capacity being grouped in a lobe in an opposing direction. The capacity of the minor axis was taken as the capacity of all slices that were not contained in the greater or lesser lobes of the major axis. The classification

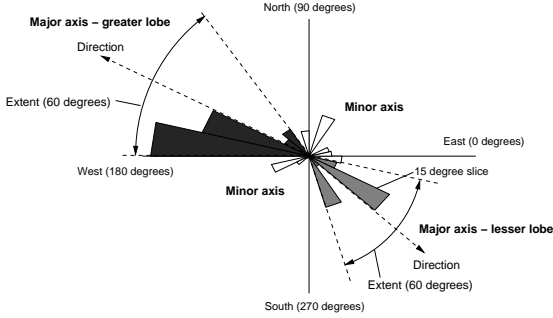


Figure 2: Classification of a hub-and-spoke network's directional capacity (Evans et al., 2010)

of the directional capacity is illustrated in Figure 2.

Two parameters are used to measure the distribution of the network's directional capacity. The parameter R_{minor_major} is defined to be the ratio of the capacity of arcs that are not along the major axis to those that are along the major axis. The parameter $R_{lesser_greater}$ is defined to be the ratio of the capacity in the lesser lobe of the major axis to the capacity in the greater lobe of the major axis. An analysis of the correlation between each arc distance CDF and the parameters measuring directional capacity showed that networks have a range of geometries and that this range varies for each arc distance CDF. Two pairs of directional capacity parameters that best represented the networks of each arc distance CDF were chosen.

The scheduled time for an aircraft leg between push back from the originating port gate and arrival at the destination port gate is known as the *block time*. This time is the sum of the taxi time on departure, flight time, and taxi time on arrival. Taxi times are relatively constant, and the flight time is approximately a linear function of the arc distance plus extra time involved in climbing and descending at lower speed. Prevailing westerly winds mean that flight times for arcs directed west to east are normally less than those for arcs directed from east to west. Arcs are categorized into two groups depending upon whether the travel direction is east-west or west-east. A linear model of block time in minutes as a function of distance in kilometres is fitted to each group.

To model time zone effects, a time zone offset is applied to ports that are at a large east-west distance from the hub. It is assumed that the hub is positioned at the equator at the centre of a one hour time zone. Assuming the mean radius of the Earth is 6371km, the width of each one hour time zone at the equator is 1668km.

In Section 4 it is explained briefly how this analysis is used to generate flight network topologies and arc passenger loads, from given parameters; full details can be found in Evans et al. (2010).

2.2. Airline transit passenger ratios

The percentage of passengers transiting through a port and connecting to another arc in the airline's network is strongly influenced by the geographical location of the ports with respect to each other. To calculate OD-pair passenger demand from

| Type | Example | θ |
|----------------|--------------------|----------|
| Point-to-point | Australia Domestic | 0.77 |
| Point-to-point | Southwest Domestic | 0.64 |
| Hub | United to/from LAX | 0.58 |
| Hub | United to/from ORD | 0.34 |
| Hub | United to/from DEN | 0.31 |
| Heavy Hub | Delta to/from ATL | 0.19 |

Table 1: Values of θ for a variety of airlines and networks (Evans, 2010)

the passenger load data, knowledge of these passenger *transit ratios* is needed. Evans (2010) compares a range of network topologies and proposes a simple generic methodology to estimate these ratios if they are not known using passenger loads and a small number of assumptions. This section provides an overview of this methodology.

Let Δ_{ij} denote the great-circle distance between any two ports $i, j \in S$, and note that $\Delta_{ii} = 0$. Let γ denote the maximum ratio of the total distance a passenger would travel between ports i and j to the direct distance between these ports. Note that there may not be any direct flights between the ports i and j , that is, $(i, j) \notin A$.

Consider the arc $(i, j) \in A$. Let θ_{ij} denote the minimum expected proportion of single-leg passengers on (i, j) . Evans suggests that, in general, the values of θ_{ij} and θ_{ji} are likely to be very similar, and, for all practical purposes, that it can be assumed that $\theta_{ij} = \theta$ where the value of θ depends upon the topology of the network. For example, values for θ_{ij} range from around 0.75 for arcs in a point-to-point network, to 0.4, or even smaller, for arcs in a hubbing network. The value of θ will decrease, the larger the hub port the arc is incident to. An exception to $\theta_{ij} = \theta$ is if an airline is not allowed to sell single-leg tickets for (i, j) in which case $\theta_{ij} = 0$. For example, United Airlines are not allowed to sell single-leg tickets for the Melbourne-Sydney leg of the route Los Angeles-Melbourne-Sydney-Los Angeles as they are not a domestic Australian airline. Table 1 gives typical values of θ for a variety of airlines and networks.

Let σ_{ij} denote the expected fraction of passengers who arrive at port j from port i and will connect to another leg. If port j is a spoke then $\sigma_{ij} = 0$. If port j is large hub then one would expect that σ_{ij} would be very close to $0.5(1 - \theta_{ij})$ unless port i is a spoke in which case $\sigma_{ij} = (1 - \theta_{ij})$. The actual value of σ_{ij} will be strongly influenced by the geographical location of the destination ports of the legs that the transiting passengers connect to via port j . Let $\alpha_{ijj'}$ denote the fraction of the transiting passengers σ_{ij} who in turn transfer to arc $(j, i') \in A$. The expected fraction of passengers who arrive at port j from port i and then connect to arc (j, i') is denoted by $\sigma_{ijj'} = \alpha_{ijj'} \sigma_{ij}$.

Transiting passengers are likely to connect to arcs $(j, i') \in A$ when port i' is in some sense geographically "opposite" to port i . Let $A_{ij}^{\text{out}} = \{(j, i') \in A : \Delta_{ij} + \Delta_{ji'} \leq \gamma \Delta_{ii'}\}$ denote the set of arcs corresponding to such *outgoing* connections. However, the arc (i, j) wont be the sole contributor of transiting passengers to these connections. The arcs $(i', j) \in A$ that are in some sense

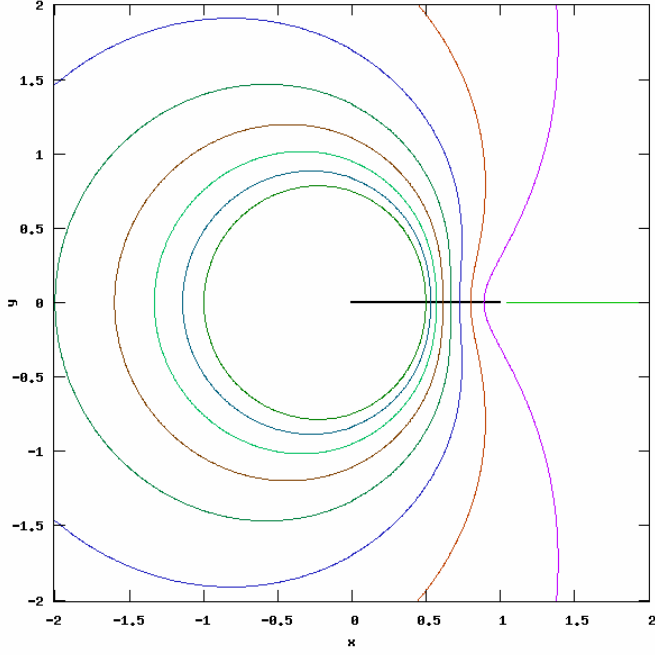


Figure 3: Contour lines for varying γ values in a normalised Euclidean space

geographically “parallel” to the arc (i, j) are also likely to contribute transiting passengers. Let $A_{ij}^{\text{in}} = \{(i', j) \in A : \Delta_{ij} + \Delta_{i'j} > \gamma \Delta_{i'j}\}$ denote the set of arcs corresponding to such *incoming* connections. Note that $(i, j) \in A_{ij}^{\text{in}}$. The maximum number of passengers transiting from arcs in A_{ij}^{in} to arcs in A_{ij}^{out} is given by

$$\min \left(\sum_{(i', j) \in A_{ij}^{\text{in}}} n_{i'j}(1 - \theta_{i'j}), \sum_{(j, i') \in A_{ij}^{\text{out}}} n_{ji'}(1 - \theta_{ji'}) \right).$$

Assuming that the same proportion of passengers over and above $\theta_{i'j}$, for each arc $(i', j) \in A_{ij}^{\text{in}}$, will connect to arcs $(j, i') \in A_{ij}^{\text{out}}$, then the expected fraction of passengers who traverse arc (i, j) and connect to another arc will be

$$\sigma_{ij} = \beta_{ij}(1 - \theta_{ij}) \min \left(1, \frac{\sum_{(j, i') \in A_{ij}^{\text{out}}} n_{ji'}(1 - \theta_{ji'})}{\sum_{(i', j) \in A_{ij}^{\text{in}}} n_{i'j}(1 - \theta_{i'j})} \right)$$

where $\beta_{ij} = 1$ if arc $(i, j) \in A_{i'i}^{\text{out}}$ for some arc $(i', i) \in A$, and $\beta_{ij} = 0.5$ otherwise.

Following an analysis of available data, Evans claims that $\alpha_{ijj'}$, the fraction of transiting passengers who connect to an arc $(j, i') \in A_{ij}^{\text{out}}$, is well approximated by

$$\alpha_{ijj'} = n_{ji'} \left(\frac{\Delta_{i'j}}{\Delta_{ij} + \Delta_{j'i'}} \right)^4 \left/ \sum_{(j, i'') \in A_{ij}^{\text{out}}} n_{ji''} \left(\frac{\Delta_{i''j}}{\Delta_{ij} + \Delta_{j'i''}} \right)^4 \right.$$

Figure 3 illustrates the effect of the choice of γ on the sets of incoming and outgoing arcs for an arc (i, j) in a normalised Euclidean space where it is assumed that port i is located at $(0, 0)$ and port j is located at $(1, 0)$. Each line emanating from port j denotes a contour of the function $\Delta_{ij} + \Delta_{j'i'} = \gamma \Delta_{i'j}$ for $\gamma = \{1, 1.25, 1.5, \dots, 3\}$.

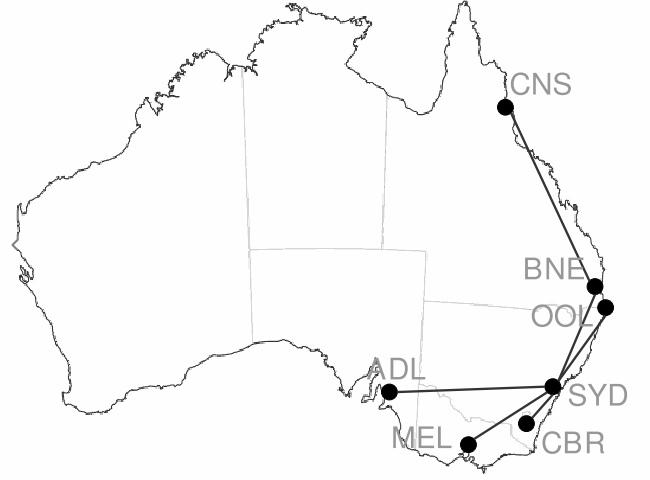


Figure 4: An example hub-and-spoke network

| Ports | ADL | BNE | CBR | CNS | MEL | OOL | SYD |
|-------|------|------|------|------|------|------|------|
| ADL | - | 1621 | 971 | 2132 | 642 | 1604 | 1165 |
| BNE | 1621 | - | 956 | 1392 | 1381 | 95 | 752 |
| CBR | 971 | 956 | - | 2076 | 469 | 892 | 237 |
| CNS | 2132 | 1392 | 2076 | - | 2313 | 1485 | 1971 |
| MEL | 642 | 1381 | 469 | 2313 | - | 1329 | 706 |
| OOL | 1604 | 95 | 892 | 1485 | 1329 | - | 679 |
| SYD | 1165 | 752 | 237 | 1971 | 706 | 679 | - |

Table 2: Great-circle distances in kilometres between any pair of ports in the example network

| Ports | ADL | BNE | CBR | CNS | MEL | OOL | SYD |
|-------|------|------|-----|-----|-----|-----|------|
| ADL | - | 0 | 0 | 0 | 0 | 0 | 975 |
| BNE | 0 | - | 0 | 480 | 0 | 0 | 1477 |
| CBR | 0 | 0 | - | 0 | 0 | 0 | 486 |
| CNS | 0 | 519 | 0 | - | 0 | 0 | 0 |
| MEL | 0 | 0 | 0 | 0 | - | 0 | 776 |
| OOL | 0 | 0 | 0 | 0 | 0 | - | 222 |
| SYD | 1120 | 1466 | 538 | 0 | 798 | 214 | - |

Table 3: Passenger loads for the example network

Example. Consider the hub-and-spoke network given in Figure 4. Table 2 gives the great-circle distance between any pair of ports regardless of whether there exists an arc in the network. Table 3 gives the passenger load on each arc in the network.

The port SYD is a single hub. Each of the ports ADL, CBR, MEL, and OOL, have a direct connection to only one other port, namely the hub SYD. Each of these ports and the hub form a simple spoke. The port CNS and the hub form a spoke with an intermediate stop, namely BNE, which lies approximately on the same flight path.

In the case of a hub-and-spoke network, passengers wishing to travel from one spoke port to another must transit through the hub. Thus, the percentage of passengers transiting through the hub SYD and connecting to another arc will be high. No passengers arriving at the spoke ports ADL, CBR, CNS, MEL, and OOL, will connect to another arc. There are likely to be a high number of transit passengers at the intermediate stop BNE.

If the distance between spoke ports is much shorter than the total distance to be travelled when connecting via the hub, for example, BNE and OOL, then travellers will not connect between these ports via the hub, instead preferring to use some alternate method of transport.

Suppose $\gamma = 2$ and $\theta_{ij} = 0.4$ for all $(i, j) \in A$. Consider the arc (SYD, BNE). The set $A_{\text{SYD,BNE}}^{\text{in}} = \{(\text{SYD}, \text{BNE})\}$, $A_{\text{SYD,BNE}}^{\text{out}} = \{(\text{BNE}, \text{CNS})\}$, and

$$\sigma_{\text{SYD,BNE}} = (1 - 0.4) \min \left(1, \frac{(1 - 0.4)480}{(1 - 0.4)1466} \right) \approx 0.196.$$

Consider the arc (OOL, SYD). The set $A_{\text{OOL,SYD}}^{\text{in}} = \{(\text{BNE}, \text{SYD}), (\text{OOL}, \text{SYD})\}$, $A_{\text{OOL,SYD}}^{\text{out}} = \{(\text{SYD}, \text{ADL}), (\text{SYD}, \text{CBR}), (\text{SYD}, \text{MEL})\}$, $\sigma_{\text{OOL,SYD}} = (1 - 0.4) = 0.6$,

$$\begin{aligned} \alpha_{\text{OOL,SYD,ADL}} &= \frac{1120 \left(\frac{1604}{679+1165} \right)^4}{1120(0.870)^4 + 538(0.974)^4 + 798(0.960)^4} \\ &= \frac{641.197}{1801.548} \approx 0.356 \end{aligned}$$

and $\sigma_{\text{OOL,SYD,ADL}} \approx 0.214$.

The transit ratios resulting from the above analysis are critical to the deduction of OD-pair demand from observed passenger loads on arcs, a process discussed in detail in the next section.

3. Characterising airline demand using limited data

Accurate passenger demand data is vitally important to the design of a good airline schedule and to the subsequent fleet assignment. Typically airlines only have data about passenger numbers on flights at the times that these have occurred in the past, rather than information about when passengers would most like to fly. Revenue management initiatives, a lack of capacity at peak times, and portions of the network with a low number of services per day, all contribute to passengers not flying at their preferred times.

A further complication is that it is difficult to infer OD-pair demand from such data for a number of reasons. Often it is

the case that a passenger's actual origin and destination is not known to the airline. Even when booked passenger itinerary data is available, from an airline reservation system for example, the data will not reflect the true demand in cases where infrequent services or bad connections force passengers to break their trip at an intermediate port, and when passengers book legs separately, or use another carrier for some legs.

Whilst a great deal is known about inferring features of OD demand from observed arc demand in road networks (see, for example, Florian (1976)), nothing of this type has yet been attempted for airlines.

3.1. Calculating arc passenger data

Airlines often have data on historical or forecast passenger numbers for directly connected port pairs. However, if arc passenger data is not known, it can often be obtained from data that is available, and averaging data taken from multiple days can reduce the effects of the frequency of services.

For example, if complete daily flight schedules with passenger numbers for each flight are available, then passenger load can be calculated by averaging the number of passengers over all days and all flights between the two ports in the direction of the arc. If the number of passengers for a flight is not known, then this can be estimated using the capacity of the aircraft assigned to the flight along with an estimate of the average percentage of occupied seats, or *load factor*.

3.2. Calculating OD-pair demand data

Calculating OD-pair demand that is compatible with the observed passenger loads on each arc requires the solution of a type of inverse problem. This problem is modelled as a path-based multicommodity flow problem and requires the identification of all possible paths passengers may take between each OD-pair. Two objectives are considered. The first is the deviation from the expected transit ratios. The second is the level of asymmetry in the OD-pair passenger demand. As it is not clear what the trade-off is between these two objectives, a biobjective model is considered.

Characterising reasonable OD-paths. There may be many potential paths between an OD-pair $(o, d) \in \bar{K}$ in the flight network. However, not all of them will be considered *reasonable* with respect to the distance travelled from o to d , the time taken, the number of connections required, or the path's subpaths.

The distance travelled on a path between the OD-pair (o, d) is the sum of the great-circle distances of the arcs on the path. A path p is reasonable with respect to the distance travelled if

$$\sum_{a \in \mathcal{A}_p} \Delta_a \leq \gamma \Delta_{od}$$

where \mathcal{A}_p denotes the set of arcs on path p .

The time taken on a path is estimated to be the average waiting time plus the block time. The average waiting time w_{ij} for an arc $(i, j) \in A$ is estimated to be half the expected time between flights. If c_{max} denotes the largest aircraft capacity, then a lower bound on the number of aircraft operating on the arc

$(i, j) \in A$ is $\mathcal{N}_{ij} = n_{ij}/c_{\max}$. Thus, the expected waiting time between flights is $\mathcal{T}/\mathcal{N}_{ij}$, and $w_{ij} = 0.5\mathcal{T}/\mathcal{N}_{ij}$. Let t_{ij} denote the block time.

The time taken between the OD-pair (o, d) is measured with respect to the time $w_{p_{\min}} + t_{p_{\min}}$ taken to travel the great-circle shortest-distance path p_{\min} . A path p is reasonable with respect to the time taken if

$$\sum_{(i,j) \in \mathcal{A}_p} (w_{ij} + t_{ij}) \leq w_{p_{\min}} + t_{p_{\min}}$$

For the short- and medium-haul networks considered in this paper it is assumed that the maximum number of connections on a reasonable path is two. That is, the number of arcs on a reasonable path is at most three. Note that limiting the number of connections is a practical consideration. The methodology described in this paper works for an arbitrary number of connections on a path.

A path p is reasonable with respect to its subpaths if all subpaths are reasonable.

Example. Suppose that the arc (MEL, BNE) with 466 passengers per day also exists in the example network. Since (MEL, BNE) is an arc, it is the shortest-distance path for this OD-pair. Consider the path MEL – SYD – BNE and suppose that the biggest aircraft has a capacity for 160 passengers. The expected number of aircraft on each leg is $\mathcal{N}_{\text{MEL,SYD}} = 776/160 = 4.85$, $\mathcal{N}_{\text{SYD,BNE}} = 752/160 = 4.7$, $\mathcal{N}_{\text{MEL,BNE}} = 466/160 = 2.9125$. The average waiting time in minutes for each arc is $w_{\text{MEL,SYD}} = 0.5 \times 1440/4.85 = 148$, $w_{\text{SYD,BNE}} = 0.5 \times 1440/4.7 = 153$, $w_{\text{MEL,BNE}} = 0.5 \times 1440/2.9125 = 247$. The block times in minutes for each arc is $t_{\text{MEL,SYD}} = 65$, $t_{\text{SYD,BNE}} = 68$, $t_{\text{MEL,BNE}} = 112$. Since $148 + 65 + 153 + 68 > 247 + 112$, MEL – SYD – BNE is not a reasonable path.

A path-based biobjective multicommodity flow model. Let $\mathcal{P}^k = \{p_1, p_2, \dots, p_{|\mathcal{P}^k|}\}$ denote all reasonable paths between each OD-pair $k \in \bar{K}$ ordered by nondecreasing time taken. Let the parameter η_k denote a normalization factor for the demand for OD-pair $k \in \bar{K}$, so that OD-pair penalties in the optimisation model below are comparable across OD-pairs. The maximum number of passengers that can transit from arc $(i, j) \in A$ to arc $(j, i') \in A_{ij}^{\text{out}}$ is $n_{ijj'} = \min(n_{ij}, n_{j'})$.

Let the variable x_p denote the number of passengers on path $p \in \mathcal{P}^k$ between OD-pair $k \in \bar{K}$. The variable ψ_{od} measures any excess in demand between OD-pair $(o, d) \in \bar{K}$ over that of (d, o) , relative to η_{od} . The value of η_{od} is set so as to be a guaranteed “tight” upper bound on the OD-pair demand for (o, d) . It is “tight” in the sense that there exists a feasible solution achieving the bound. This ensures that all ψ_{od} values will be in the range $[0, 1]$. The variable $\epsilon_{ijj'}$ measures the deviation from the expected transit ratio $\sigma_{ijj'}$ for arcs $(i, j) \in A$ and $(j, i') \in A_{ij}^{\text{out}}$.

The biobjective multicommodity flow (MCF) model is formulated as follows.

$$\min \begin{cases} \sum_{\substack{(o,d) \in \bar{K}: \\ o < d}} (\psi_{od} + \psi_{do})^2 \\ \sum_{(i,j) \in A} \sum_{(j,i') \in A_{ij}^{\text{out}}} \epsilon_{ijj'}^2 \end{cases} \quad (1)$$

$$\text{s.t. } \sum_{k \in \bar{K}} \sum_{\substack{p \in \mathcal{P}^k: \\ a \in \mathcal{A}_p}} x_p = n_a, \quad a \in A \quad (2)$$

$$\sum_{p \in \mathcal{P}^{(o,d)}} x_p - \sum_{p \in \mathcal{P}^{(d,o)}} x_p \leq \eta_{od} \psi_{od}, \quad (o, d) \in \bar{K} \quad (3)$$

$$\epsilon_{ijj'} = \sigma_{ijj'} - \sum_{\substack{(o,d) \in \bar{K}: \\ d \neq j}} \sum_{\substack{p \in \mathcal{P}^{(o,d)}: \\ (i,j) \in \mathcal{A}_p}} \frac{x_p}{n_{ijj'}}, \quad (i, j) \in A, (j, i') \in A_{ij}^{\text{out}} \quad (4)$$

$$x_p \geq x_{p_{r+1}}, \quad r \in \{1, 2, \dots, |\mathcal{P}^k|\}, k \in \bar{K} \quad (5)$$

$$x_p, \psi_k \geq 0, \quad p \in \mathcal{P}^k, k \in \bar{K} \quad (6)$$

The two objectives (1), asymmetry in passenger flow and deviation from the expected transit ratios, are measured by minimising the sum of the squares of the individual terms. Quadratic, rather than linear, penalties are chosen in order to reduce the likelihood of outliers. Constraints (2) ensures that the passenger load on each arc is met exactly. Constraints (3) and (4) measure the asymmetry in passenger flow and the deviation from the expected transit ratios respectively. Constraints (5) ensure that more reasonable paths have a larger number of passengers. Constraints (6) ensure nonnegativity of the x_p and ψ_k variables.

The feasible set of solutions to this problem is nonempty. For each feasible solution there is a corresponding set $K \subseteq \bar{K}$ of OD-pairs with nonzero passenger demand. The corresponding feasible set of points in objective space is convex. There are infinitely many efficient solutions in decision space and, correspondingly, infinitely many nondominated points in objective space.

It is not clear what the trade-off is between the two objective functions. Each decision maker will place a different importance on each of the objectives and so identify different efficient solutions as the best solution for their needs. In order to aid the decision maker in this choice an inner piecewise linear approximation to the actual frontier can be obtained by sampling nondominated points. Each nondominated point can be determined by solving the MCF model with a single quadratic objective obtained by taking a weighted combination of the two objective functions using regularly spaced weights chosen from the unit interval.

4. Benchmark instances

The benchmark instances consist of thirty single-hub and three two-hub networks. Tables 4 and 5 provide the parameters used to generate the networks. In these tables the hub name is preceded by either an “s”, “m”, or “l”, indicating whether the instance is considered to be a short-, medium-, or long-haul network, respectively.

To generate a single-hub network having a given number of spokes, the network characteristics identified in Section 2.1 are used. Recall that five possible arc distance CDFs and five possible arc capacity CDFs were identified. Which of these is used for an instance is indicated in Table 4, by index. Details of the CDF corresponding to each index can be found in Evans et al. (2010). For each spoke, first the length of the spoke is sampled

| Hub name | Distance CDF | Capacity CDF | R_{minor_major} | | $R_{lesser_greater}$ | | Spoke ports | Spoke capacity | | Inter-hub capacity | | Multi-hub spoke ports | Inter-hub distance |
|----------|--------------|--------------|--------------------|--------|-----------------------|--------|-------------|----------------|--------|--------------------|--------|-----------------------|--------------------|
| | | | Target | Actual | Target | Actual | | Target | Actual | Target | Actual | | |
| sHAB | 2 | 4 | 0.2 | 0.19 | 0.75 | 0.75 | 18 | 0.4 | 0.39 | 0.013 | 0.013 | 14 | 1400 |
| sHBB | | | 0.1 | 0.07 | 0.55 | 0.65 | 20 | 0.59 | 0.60 | | | | |
| sHCB | 2 | 4 | 0.2 | 0.25 | 0.75 | 0.73 | 54 | 0.40 | 0.42 | 0.013 | 0.012 | 42 | 1400 |
| sHDB | | | 0.1 | 0.15 | 0.55 | 0.46 | 60 | 0.59 | 0.57 | | | | |
| sHEB | 2 | 4 | 0.2 | 0.15 | 0.75 | 0.76 | 90 | 0.40 | 0.38 | 0.013 | 0.012 | 70 | 1400 |
| sHFB | | | 0.1 | 0.18 | 0.55 | 0.5 | 100 | 0.59 | 0.61 | | | | |

Table 5: Parameters for generating two-hub benchmark instances

| Hub name | Distance CDF | Capacity CDF | R_{minor_major} | | $R_{lesser_greater}$ | | Spoke ports |
|----------|--------------|--------------|--------------------|--------|-----------------------|--------|-------------|
| | | | Target | Actual | Target | Actual | |
| sHAA | 1 | 4 | 0.4 | 0.43 | 0.4 | 0.43 | 24 |
| sHBA | | | 0.4 | 0.44 | 0.4 | 0.43 | 72 |
| sHCA | | | 0.4 | 0.43 | 0.4 | 0.42 | 120 |
| sHDA | 1 | 4 | 0.8 | 0.77 | 0.4 | 0.41 | 24 |
| sHEA | | | 0.8 | 0.79 | 0.4 | 0.43 | 72 |
| sHFA | | | 0.8 | 0.81 | 0.4 | 0.44 | 120 |
| sHGA | 2 | 4 | 0.2 | 0.23 | 0.4 | 0.43 | 24 |
| sHHA | | | 0.2 | 0.22 | 0.4 | 0.42 | 72 |
| sHIA | | | 0.2 | 0.23 | 0.4 | 0.42 | 120 |
| sHJA | 2 | 4 | 0.4 | 0.43 | 0.8 | 0.81 | 24 |
| sHKA | | | 0.4 | 0.42 | 0.8 | 0.8 | 72 |
| sHLA | | | 0.4 | 0.42 | 0.8 | 0.8 | 120 |
| mHMA | 3 | 4 | 0.2 | 0.23 | 0.2 | 0.23 | 12 |
| mHNA | | | 0.2 | 0.23 | 0.2 | 0.23 | 24 |
| mHOA | | | 0.2 | 0.22 | 0.2 | 0.22 | 60 |
| mHPA | 3 | 4 | 0.2 | 0.23 | 0.8 | 0.81 | 12 |
| mHQA | | | 0.2 | 0.23 | 0.8 | 0.81 | 24 |
| mHRA | | | 0.2 | 0.21 | 0.8 | 0.79 | 60 |
| IHSA | 4 | 5 | 0.1 | 0.12 | 0.5 | 0.55 | 12 |
| IHTA | | | 0.1 | 0.13 | 0.5 | 0.53 | 24 |
| IHUA | | | 0.1 | 0.12 | 0.5 | 0.51 | 60 |
| IHVA | 4 | 5 | 0.5 | 0.53 | 0.8 | 0.78 | 12 |
| IHWA | | | 0.5 | 0.52 | 0.8 | 0.8 | 24 |
| IHXA | | | 0.5 | 0.5 | 0.8 | 0.78 | 60 |
| IHYA | 5 | 5 | 0.2 | 0.22 | 0.1 | 0.14 | 12 |
| IHZA | | | 0.2 | 0.22 | 0.1 | 0.12 | 24 |
| IH1A | | | 0.2 | 0.23 | 0.1 | 0.13 | 72 |
| IH2A | 5 | 5 | 0.1 | 0.11 | 0.7 | 0.67 | 12 |
| IH3A | | | 0.1 | 0.14 | 0.7 | 0.72 | 24 |
| IH4A | | | 0.1 | 0.13 | 0.7 | 0.72 | 72 |

Table 4: Parameters for generating single-hub benchmark instances

from the given arc distance CDF, and then its capacity is sampled from the given capacity CDF. Then the directions of all spokes are determined, so as to match the lobe characteristics described in Section 2.1, and quantified by the R_{minor_major} and $R_{lesser_greater}$ values given in Table 4. Target and actual values are given for these directional capacity parameters. For each combination of arc distance CDF, arc capacity CDF, and target directional capacity parameters, three networks of different sizes were generated in order to allow for the investigation of scaling effects.

The two-hub instances were generated by “glueing” two single-hub instances together in an acceptable way. Table 5 contains the additional parameters needed in order to generate the two-hub networks. The spoke capacity and inter-hub capacity columns provide the fraction of the total number of passengers in the network that are observed on each hub’s spoke arcs and the inter-hub arc. The multi-hub spoke ports column provides the number of spoke ports that the two hubs have in common. The inter-hub distance is the number of kilometres that the second hub lies to east of the first.

In generating OD-pair demands, the nominal value used for the expected proportion of single-leg passengers on any arc was $\theta = 0.3$ for short-haul networks and $\theta = 0.6$ for both medium- and long-haul. The maximum ratio of the total distance a passenger would travel between ports to the direct distance between these ports used for all instances was $\gamma = 2$.

The complete set of instances and supporting material is available at the URL http://www.infotech.monash.edu.au/~wallace/airline_benchmarks/ along with the references Evans (2010) and Evans et al. (2010).

5. Analysis of instances

Summary statistics are presented for all of the benchmark instances. More detailed results are presented for the previously introduced example instance, three selected single-hub instances, one two-hub instance, and a fictitious Australian carrier called Emu Airlines that operates a point-to-point network. For these instances, network and directional capacity diagrams, and plots of a sampled efficient frontier and the cumulative distribution of single-leg passengers, are presented.

On the plots of the sampled efficient frontier, open circles indicate the nondominated points corresponding to weights that are a multiple of 0.1. The dotted line connects the ideal point to the closest nondominated point measured using the L_2 -norm

| Ports | ADL | BNE | CBR | CNS | MEL | OOL | SYD |
|-------|-----|-----|-----|-----|-----|-----|-----|
| ADL | - | 293 | 47 | 0 | 0 | 28 | 607 |
| BNE | 308 | - | 136 | 332 | 189 | 0 | 650 |
| CBR | 38 | 142 | - | 0 | 0 | 3 | 284 |
| CNS | 0 | 325 | 0 | - | 0 | 0 | 194 |
| MEL | 0 | 210 | 0 | 0 | - | 3 | 537 |
| OOL | 34 | 0 | 3 | 0 | 3 | - | 128 |
| SYD | 740 | 673 | 329 | 148 | 575 | 135 | - |

Table 6: Passenger demand between OD-pairs in the example network

when the frontier is normalised to fit within a unit square. The asterisk indicates a point, identified by an industrial partner, on the efficient frontier that is an acceptable trade-off between the asymmetry in passenger flow and the deviation from the expected transit ratios. The plots of the cumulative distribution of single-leg passengers show the fraction of network arcs that have at most the given fraction of single-leg passengers. These are passengers that are flying directly between their origin and destination.

5.1. Example instance

The nominal value used for the expected proportion of single-leg passengers on any arc was $\theta = 0.3$. The maximum ratio of the total distance a passenger would travel between ports to the direct distance between these ports was $\gamma = 2$. Table 6 provides the passenger demand between OD-pairs in the example network. These demands are obtained from the efficient solution corresponding to the nondominated point identified by an industrial partner.

Figure 5 shows the frontier and single-leg passenger CDF plots. While there exists an efficient solution with no deviation from the expected transit ratios, there does not exist a solution which has no asymmetry in the passenger flows. The hub is quite asymmetrical. As a result of the asymmetry in the network’s capacity there is a significantly large proportion of single-leg passengers. The average observed proportion is just over 0.6 which is much greater than the nominal value of 0.4.

5.2. Benchmark instances

Summary statistics for the thirty single-hub and three two-hub networks are presented in Table 7. These tables summarise the number of spoke ports, network arcs, OD-pairs with nonzero demand, and passengers in the network. Statistics on the distribution of the observed number of passengers on an arc, the duration of a leg on an arc, the great-circle distance of an arc, the number of unique passenger itineraries (paths) for an OD-pair, the demand for an OD-pair, and the percentage of passengers transiting at a port, are also given. The instances are grouped into threes. Each group of three networks were generated using the same parameters except the number of spokes which was varied to provide networks of different sizes.

Single-hub benchmark instances. Three single-hub instances are presented. The instance HBA is a short-haul network with 72 spokes. Figure 6 show the network and directional capacity diagrams for this instance. The hub is quite asymmetrical. Seventy percent of the arc capacity is concentrated on the major axis which has an east-west orientation. Although the lobes of the major axis are diametrically opposed the east-orientated greater lobe has more than twice the capacity of the lesser lobe.

Figure 7 show the frontier and single-leg passenger CDF plots. Efficient solutions exist in which either there is no deviation from the expected transit ratios, or there is no asymmetry in the passenger flows. As a result of the asymmetry in the network’s capacity there is a significantly large proportion of single-leg passengers. The average observed proportion is nearly 0.55, almost twice the nominal value of 0.3 that was used for short-haul networks.

The instance HRA is a medium-haul network with 60 spokes. Figure 8 show the network and directional capacity diagrams for this instance. The hub is relatively symmetric. More than 80% of the arc capacity is concentrated on the major axis which has an east-west orientation. The lobes of the major axis are diametrically opposed with the lesser lobe having nearly 80% of the capacity of the greater lobe. The greater lobe is orientated east.

Figure 9 show the frontier and single-leg passenger CDF plots. Efficient solutions exist in which either there is no deviation from the expected transit ratios, or there is no asymmetry in the passenger flows. The observed proportion of single-leg passengers is only slightly increased over the nominal value of 0.6 that was used for medium-haul networks.

The instance HXA is a long-haul network with 60 spokes. Figure 10 show the network and directional capacity diagrams for this instance. The hub is relatively symmetric. Two-thirds of the arc capacity is concentrated on the major axis which has an east-west orientation. The lobes of the major axis are diametrically opposed with the lesser lobe having nearly 80% of the capacity of the greater lobe. The greater lobe is orientated east.

Figure 11 show the frontier and single-leg passenger CDF plots. Efficient solutions exist in which either there is no deviation from the expected transit ratios, or there is no asymmetry in the passenger flows. The observed proportion of single-leg passengers is only slightly increased over the nominal value of 0.6 that was used for long-haul networks.

Two-hub benchmark instances. The instance HCB-HDB is a network with two hubs. Figure 12 shows the network and diagram for this instance. The network has significant asymmetry. The hub HDB is located 1400km east of the hub HAB and just over 1% of the network’s passengers are observed using this arc. Forty-two of the 70 spokes are shared by the two hubs. Forty-two percent of the network’s passengers are observed travelling to spokes from HCB, while 57% are observed travelling from HDB. Eighty percent of the arc capacity of HCB is concentrated on its major axis with the lesser lobe having almost three quarters of the capacity of the greater lobe. More than 80% of the arc capacity of HDB is concentrated on its ma-

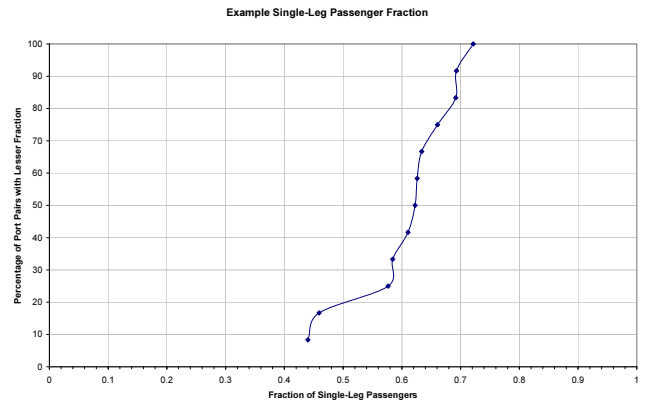
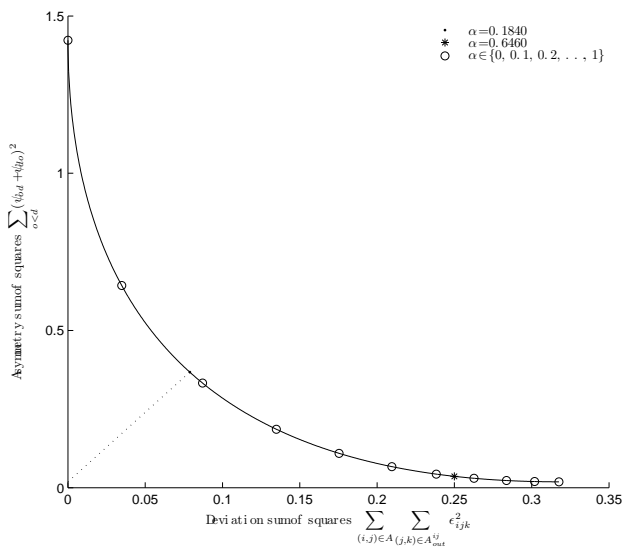


Figure 5: Frontier and single-leg passenger CDF plots for the example instance

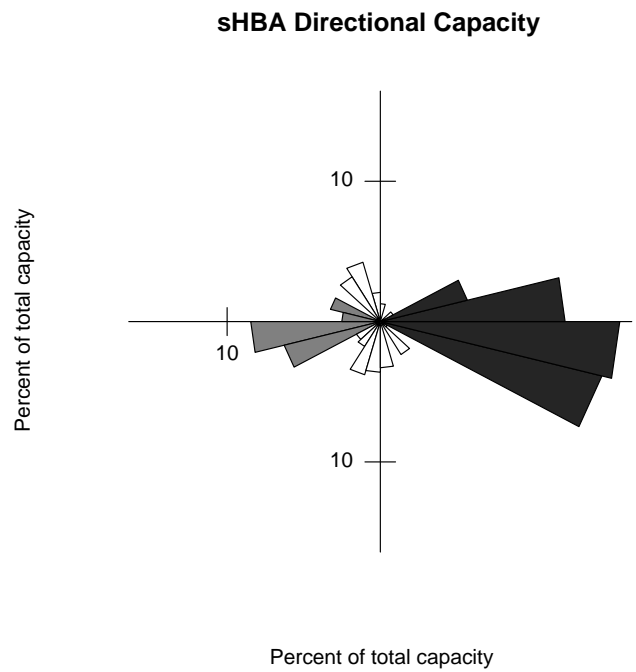
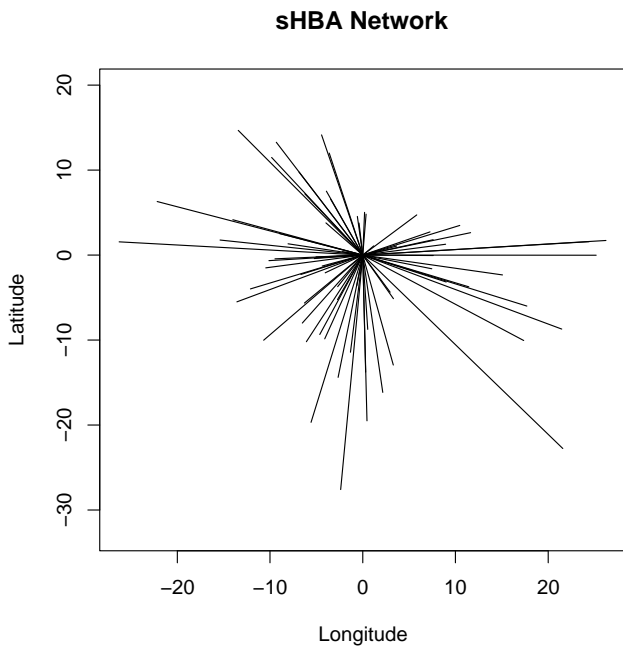


Figure 6: Network and directional capacity diagrams for the short-haul HBA instance

| Hub @name | Spoke ports | Arcs | OD pairs | Pax count | Arc pax load | | | | Block time | | | | Arc distance | | | | Origin degree | | | | OD-pair demand | | | | Transit pax % | | | |
|-----------|-------------|------|----------|-----------|--------------|---------|-----|------|------------|--------|-----|-----|--------------|---------|------|-------|---------------|-------|-----|-----|----------------|--------|-----|------|---------------|-------|-------|-------|
| | | | | | avg | stdev | min | max | avg | stdev | min | max | avg | stdev | min | max | avg | stdev | min | max | avg | stdev | min | max | avg | stdev | min | max |
| sHAA | 24 | 48 | 450 | 71410 | 1487.71 | 1340.7 | 124 | 4860 | 137.81 | 46.49 | 60 | 270 | 1338.83 | 454.88 | 249 | 3079 | 18.96 | 2.22 | 14 | 24 | 123.55 | 394.41 | 0 | 3413 | 45.81 | 11.72 | 28.51 | 70.51 |
| sHBA | 72 | 144 | 3374 | 106474 | 739.4 | 821.65 | 28 | 4860 | 135.35 | 54.42 | 55 | 300 | 1304.17 | 531.7 | 178 | 3444 | 50.88 | 10.55 | 10 | 72 | 24.38 | 140.22 | 0 | 3546 | 47.42 | 8.7 | 10.53 | 64.05 |
| sHCA | 120 | 240 | 8968 | 224898 | 937.08 | 911.61 | 68 | 4860 | 132.71 | 53.11 | 55 | 330 | 1268.03 | 520.55 | 178 | 3846 | 83.32 | 15.93 | 21 | 120 | 19.25 | 131.61 | 0 | 3637 | 48.55 | 11.66 | 11.76 | 75.58 |
| sHDA | 24 | 48 | 423 | 71410 | 1487.71 | 1340.7 | 124 | 4860 | 137.81 | 46.49 | 60 | 270 | 1338.83 | 454.88 | 249 | 3079 | 17.84 | 3.07 | 13 | 24 | 130.01 | 394.18 | 0 | 3550 | 46.07 | 12.93 | 22.92 | 73.1 |
| sHEA | 72 | 144 | 3393 | 106474 | 739.4 | 821.65 | 28 | 4860 | 135.35 | 54.42 | 55 | 300 | 1304.17 | 531.7 | 178 | 3444 | 50.6 | 10.73 | 7 | 72 | 23.84 | 135.56 | 0 | 3571 | 48.48 | 9.75 | 0 | 68.92 |
| sHFA | 120 | 240 | 8955 | 224898 | 937.08 | 911.61 | 68 | 4860 | 132.71 | 53.11 | 55 | 330 | 1268.03 | 520.55 | 178 | 3846 | 82.76 | 16.76 | 16 | 120 | 18.91 | 120.04 | 0 | 3358 | 49.23 | 8.7 | 18.52 | 68.95 |
| sHGA | 24 | 48 | 448 | 53230 | 1108.96 | 1189.57 | 83 | 4860 | 161.04 | 73.21 | 70 | 325 | 1663.79 | 717.68 | 423 | 3782 | 19.12 | 2.08 | 16 | 24 | 93.11 | 332.89 | 0 | 3461 | 45.82 | 10.55 | 28.79 | 67.67 |
| sHHA | 72 | 144 | 3254 | 104278 | 724.15 | 808.63 | 28 | 4860 | 163.23 | 70.57 | 70 | 325 | 1693.36 | 691.72 | 409 | 3782 | 48.9 | 11.2 | 3 | 72 | 25.08 | 148.78 | 0 | 3829 | 46.33 | 10.43 | 0 | 64.64 |
| sHIA | 120 | 240 | 8353 | 173132 | 721.38 | 789.65 | 36 | 4860 | 161.56 | 72.02 | 60 | 330 | 1670.18 | 706.43 | 244 | 3846 | 76.53 | 19.06 | 6 | 120 | 16.01 | 113.23 | 0 | 3554 | 47.43 | 11.06 | 4.35 | 70.82 |
| sHJA | 24 | 48 | 468 | 53230 | 1108.96 | 1189.57 | 83 | 4860 | 161.04 | 73.21 | 70 | 325 | 1663.79 | 717.68 | 423 | 3782 | 19.76 | 2.3 | 15 | 24 | 85.77 | 266.22 | 0 | 2765 | 47.13 | 5.86 | 36.67 | 59.84 |
| sHKA | 72 | 144 | 3333 | 104278 | 724.15 | 808.63 | 28 | 4860 | 163.23 | 70.57 | 70 | 325 | 1693.36 | 691.72 | 409 | 3782 | 49.97 | 11.56 | 8 | 72 | 23.7 | 123.13 | 0 | 3226 | 47.1 | 7.38 | 0 | 57.95 |
| sHLA | 120 | 240 | 8283 | 173132 | 721.38 | 789.65 | 36 | 4860 | 161.56 | 72.02 | 60 | 330 | 1670.18 | 706.43 | 244 | 3846 | 76.15 | 21.28 | 5 | 120 | 15.7 | 96.26 | 0 | 3033 | 47.14 | 7.58 | 0 | 60.09 |
| mHMA | 12 | 24 | 104 | 17564 | 731.83 | 810.76 | 50 | 2640 | 278.33 | 140.98 | 70 | 555 | 3295.33 | 1378.39 | 401 | 6857 | 8.31 | 2.46 | 3 | 12 | 155.86 | 447.9 | 0 | 2506 | 19.73 | 11.86 | 5.04 | 46.56 |
| mHNA | 24 | 48 | 426 | 27824 | 579.67 | 643.89 | 45 | 2640 | 259.69 | 159.29 | 70 | 555 | 3036.79 | 1559.24 | 401 | 6859 | 17.76 | 3.71 | 7 | 24 | 57.67 | 228.21 | 0 | 2203 | 26.09 | 6.4 | 13.87 | 39.77 |
| mHOA | 60 | 120 | 1851 | 51246 | 427.05 | 479.21 | 15 | 2640 | 252.96 | 146.21 | 65 | 620 | 2941.65 | 1432.26 | 300 | 7748 | 32.39 | 12.92 | 1 | 60 | 24.47 | 132.77 | 0 | 2245 | 24.52 | 10.31 | 0 | 44.29 |
| mHPA | 12 | 24 | 120 | 17564 | 731.83 | 810.76 | 50 | 2640 | 278.33 | 140.98 | 70 | 555 | 3295 | 1377.96 | 401 | 6853 | 9.69 | 1.59 | 7 | 12 | 124.2 | 319.38 | 0 | 1817 | 26.92 | 3.81 | 20.41 | 33.32 |
| mHQA | 24 | 48 | 410 | 27824 | 579.67 | 643.89 | 45 | 2640 | 259.69 | 159.29 | 70 | 555 | 3036.88 | 1559.32 | 401 | 6859 | 17.6 | 4.34 | 5 | 24 | 58.64 | 212.9 | 0 | 2026 | 26.09 | 4.02 | 14.89 | 33.95 |
| mHRA | 60 | 120 | 1821 | 51246 | 427.05 | 479.21 | 15 | 2640 | 252.96 | 146.21 | 65 | 620 | 2941.67 | 1432.26 | 300 | 7747 | 32.33 | 12.79 | 1 | 60 | 24.29 | 121.89 | 0 | 2116 | 24.86 | 6.93 | 0 | 35.2 |
| IHSA | 12 | 24 | 127 | 20062 | 835.92 | 403.54 | 253 | 1472 | 460.42 | 231.24 | 85 | 740 | 5831.17 | 2263.04 | 619 | 9295 | 9.85 | 1.46 | 8 | 12 | 133.04 | 245.93 | 0 | 1100 | 31.01 | 4.87 | 25.32 | 42.35 |
| IHTA | 24 | 48 | 435 | 23740 | 494.58 | 281.04 | 30 | 1472 | 446.35 | 240.19 | 90 | 840 | 5628.5 | 2353.9 | 664 | 10635 | 17.76 | 3.49 | 6 | 24 | 46.41 | 132.81 | 0 | 1234 | 30.88 | 8.68 | 4 | 47.41 |
| IHUA | 60 | 120 | 2323 | 56192 | 468.27 | 256.74 | 155 | 1472 | 479.75 | 217.37 | 90 | 865 | 6090.78 | 2127.48 | 731 | 10990 | 41.11 | 6.3 | 32 | 60 | 20.64 | 86.58 | 0 | 1236 | 30.47 | 6.18 | 16.03 | 43.45 |
| IHVA | 12 | 24 | 136 | 20062 | 835.92 | 403.54 | 253 | 1472 | 460.63 | 231.33 | 85 | 740 | 5831.75 | 2263.32 | 619 | 9295 | 10.62 | 1.15 | 9 | 12 | 122.86 | 229.55 | 0 | 1052 | 31.89 | 5.4 | 23.02 | 46.04 |
| IHWA | 24 | 48 | 441 | 23740 | 494.58 | 281.04 | 30 | 1472 | 444.06 | 237.17 | 90 | 840 | 5597.75 | 2324.97 | 664 | 10635 | 17.92 | 3.65 | 6 | 24 | 45.32 | 124.89 | 0 | 1126 | 31.49 | 6.72 | 7.69 | 43.24 |
| IHXA | 60 | 120 | 2466 | 56192 | 468.27 | 256.74 | 155 | 1472 | 478.5 | 215.94 | 90 | 885 | 6074.42 | 2113.71 | 731 | 11226 | 43.7 | 6.41 | 32 | 60 | 19.13 | 78.79 | 0 | 1154 | 31.49 | 3.88 | 21.5 | 41.55 |
| IHYA | 12 | 24 | 100 | 14160 | 590 | 327.26 | 212 | 1472 | 584.79 | 144.67 | 360 | 825 | 7555.58 | 1406.59 | 4597 | 10452 | 7.69 | 2.61 | 5 | 12 | 130.34 | 260.62 | 1 | 1374 | 19.24 | 11.7 | 6.66 | 37.53 |
| IHZA | 24 | 48 | 298 | 23232 | 484 | 290.63 | 30 | 1472 | 575.73 | 130.72 | 235 | 790 | 7434.71 | 1265.08 | 2819 | 10008 | 12.16 | 5.68 | 6 | 24 | 72.46 | 190.52 | 0 | 1406 | 16.95 | 12.79 | 4.48 | 44.67 |
| IH1A | 72 | 144 | 2496 | 72408 | 502.83 | 285.21 | 107 | 1472 | 581.01 | 143.01 | 165 | 905 | 7500.85 | 1385.23 | 1817 | 11521 | 36.3 | 12.66 | 10 | 72 | 26.8 | 120.64 | 0 | 1396 | 18.96 | 12.43 | 5.23 | 45.61 |
| IH2A | 12 | 24 | 106 | 14160 | 590 | 327.26 | 212 | 1472 | 586.88 | 147.54 | 360 | 825 | 7584.5 | 1433.49 | 4597 | 10437 | 8.15 | 1.46 | 6 | 12 | 114.53 | 212.47 | 2 | 1219 | 29.86 | 6.31 | 17.19 | 39.51 |
| IH3A | 24 | 48 | 359 | 23232 | 484 | 290.63 | 30 | 1472 | 575.94 | 130.98 | 235 | 790 | 7435.12 | 1265.09 | 2819 | 9981 | 14.64 | 3.61 | 7 | 24 | 55.36 | 140.01 | 0 | 1139 | 29.39 | 4.83 | 20 | 37.24 |
| IH4A | 72 | 144 | 2834 | 72408 | 502.83 | 285.21 | 107 | 1472 | 580.59 | 142.15 | 165 | 885 | 7495.57 | 1376.48 | 1817 | 11228 | 41.12 | 6.98 | 25 | 72 | 21.89 | 93.13 | 0 | 1201 | 29.19 | 5.06 | 17.94 | 39.06 |

| Hub name | Spoke ports | Arcs | OD pairs | Pax count | Arc pax load | | | | Block time | | | | Arc distance | | | | Origin degree | | | | OD-pair demand | | | | Transit pax % | | | |
|----------|-------------|------|----------|-----------|--------------|---------|-----|------|------------|-------|-----|-----|--------------|--------|-----|------|---------------|-------|-----|-----|----------------|--------|-----|------|---------------|-------|-----|-------|
| | | | | | avg | stdev | min | max | avg | stdev | min | max | avg | stdev | min | max | avg | stdev | min | max | avg | stdev | min | max | avg | stdev | min | max |
| sHAB | 22 | 74 | 443 | 94290 | 1274.19 | 1030.61 | 167 | 4860 | 175 | 75.59 | 65 | 325 | 1854.41 | 742.25 | 300 | 3795 | 19 | 3.06 | 12 | 23 | 167.98 | 374.56 | 0 | 3530 | 40.66 | 11.06 | 2.2 | 68.31 |
| sHCB | 70 | 226 | 3340 | 184406 | 815.96 | 888.14 | 25 | 4860 | 168.65 | 80.25 | 60 | 375 | 1767.53 | 786.96 | 290 | 4459 | 50.17 | 10.6 | 8 | 71 | 44.83 | 210.97 | 0 | 3998 | 36.99 | 13.98 | 0 | 82.19 |
| SHEB | 118 | 378 | 8315 | 287234 | 759.88 | 825.93 | 35 | 4860 | 169.83 | 78.24 | 55 | 405 | 1783.7 | 767.31 | 216 | 4835 | 78.52 | 19.75 | 31 | 119 | 27.92 | 157.04 | 0 | 3537 | 36.35 | 13.66 | 0 | 75.67 |

Table 7: Summary statistics for single-hub (top) and two-hub (bottom) benchmark instances

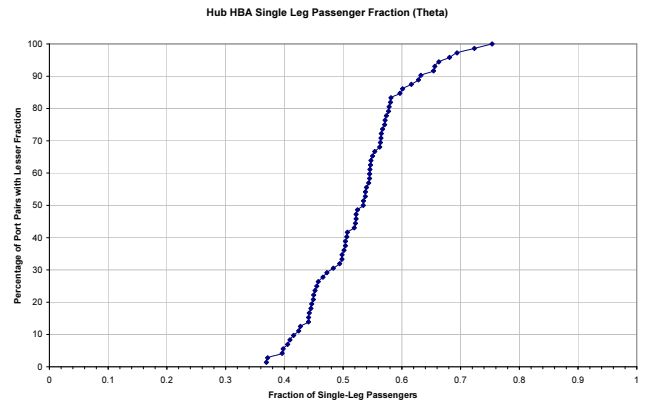
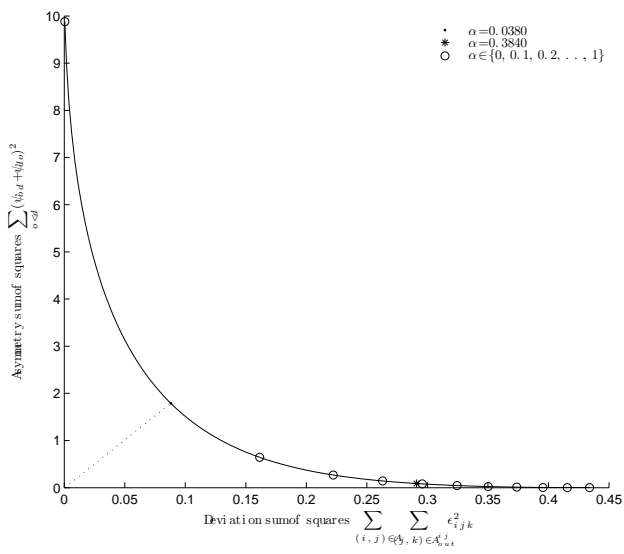


Figure 7: Frontier and single-leg passenger CDF plots for the short-haul HBA instance

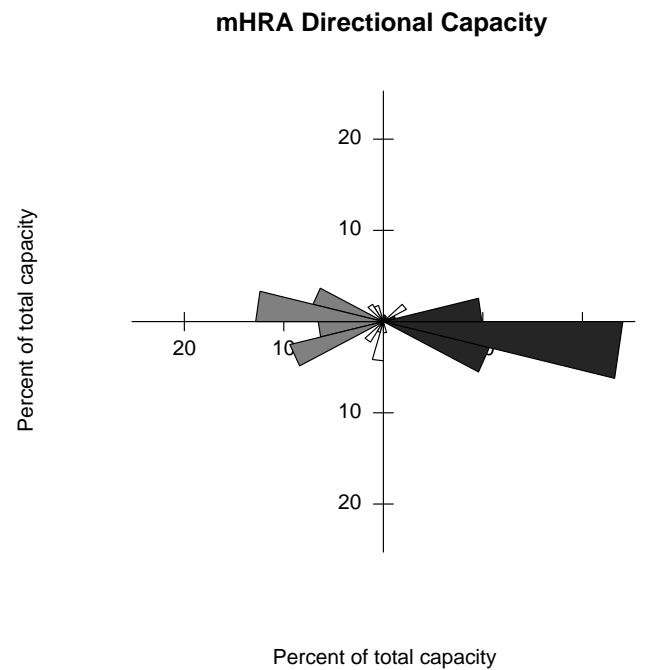
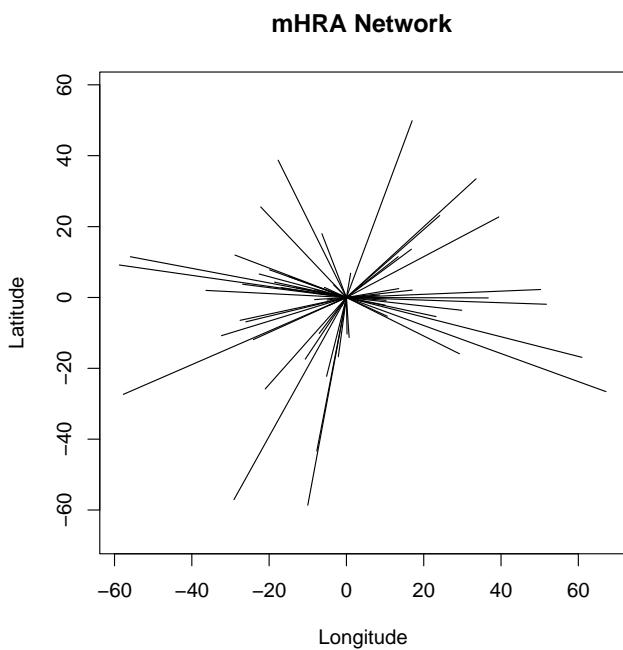


Figure 8: Network and directional capacity diagrams for the medium-haul HRA instance

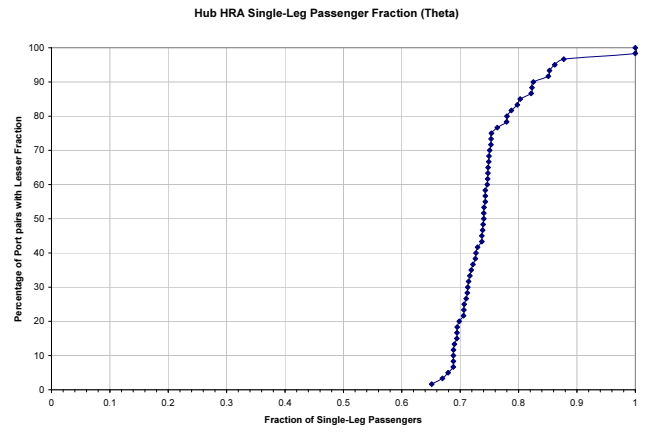
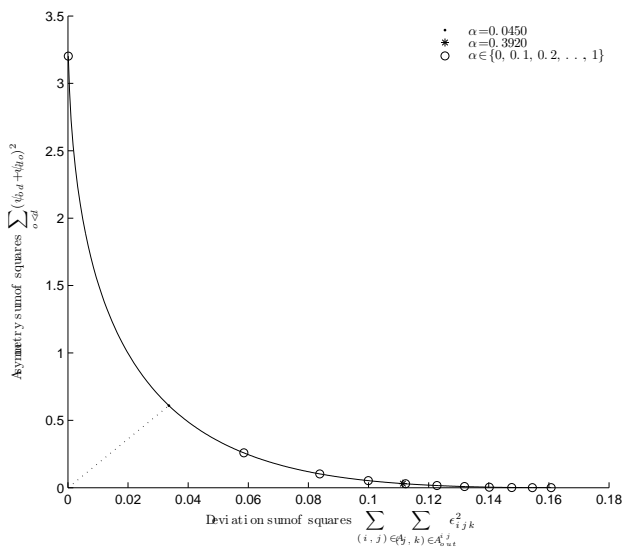


Figure 9: Frontier and single-leg passenger CDF plots for the medium-haul HRA instance

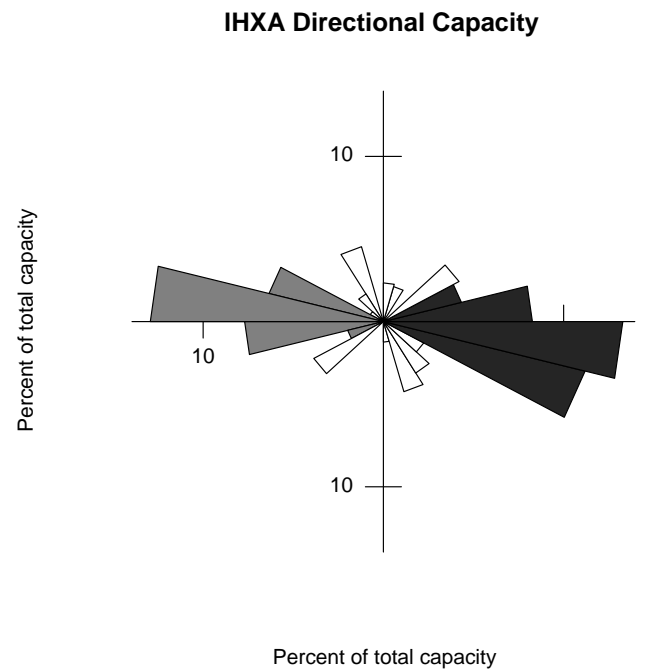
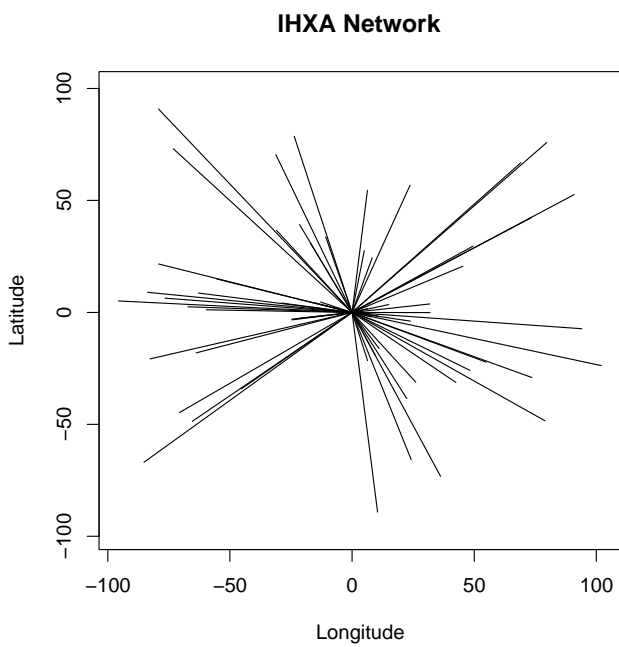


Figure 10: Network and directional capacity diagrams for the long-haul HXA instance

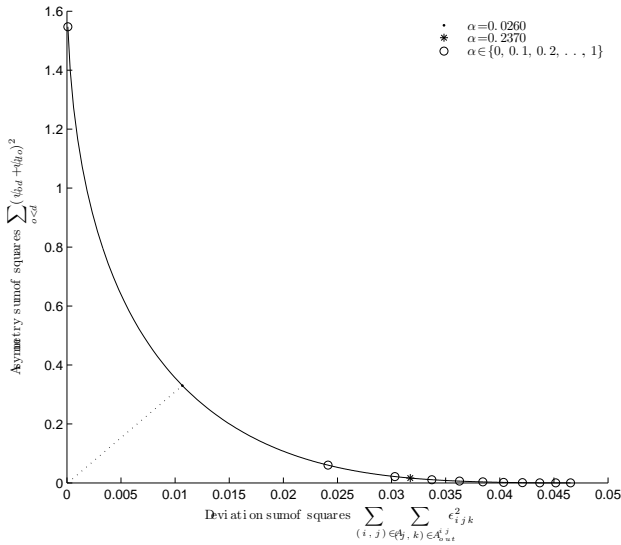


Figure 11: Frontier and single-leg passenger CDF plots for the long-haul HXA instance

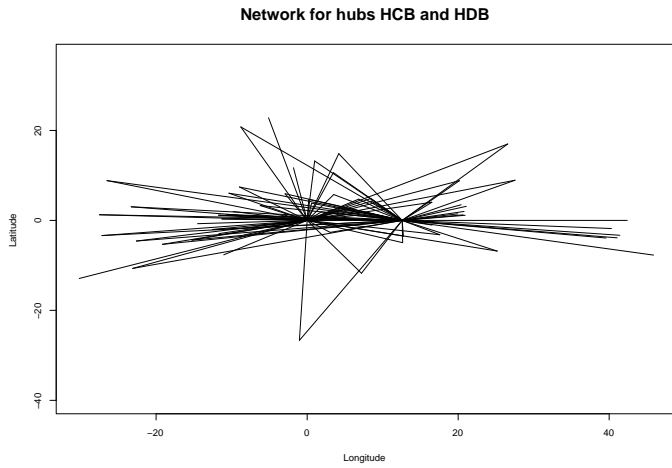
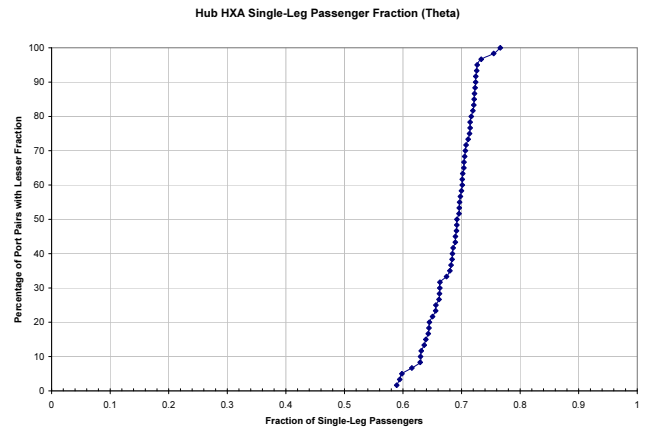


Figure 12: Network diagram for the HCB-HDB instance

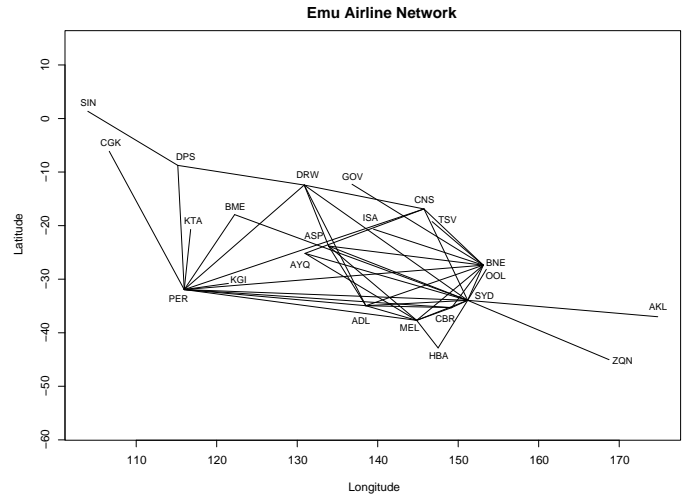


Figure 14: Point-to-point network for the Emu Airlines instance

por axis with the greater lobe having slightly more than twice the capacity of the lesser lobe.

Figure 13 show the frontier and single-leg passenger CDF plots. Efficient solutions exist in which either there is no deviation from the expected transit ratios, or there is no asymmetry in the passenger flows. As a result of the asymmetry in the network's capacity there is a significantly large proportion of single-leg passengers. The average observed proportion exceeds 0.6 which is twice the nominal value of 0.3 that was used for short-haul networks.

5.3. Point-to-point Emu Airlines instance

Emu Airlines is a fictitious Australian carrier that operates the point-to-point network shown in Figure 14. The observed passenger numbers on each arc used in this instance are based on proprietary data made available by an industrial partner.

The nominal value used for the expected proportion of single-leg passengers on any arc was $\theta = 0.75$. The maximum ratio

of the total distance a passenger would travel between ports to the direct distance between these ports used was $\gamma = 2$. Figure 15 show the frontier and single-leg passenger CDF plots. No efficient solutions exist in which either there is no deviation from the expected transit ratios, or there is no asymmetry in the passenger flows. As a result of the network being predominantly point-to-point and a quite high nominal value for θ , the observed proportion of single-leg passengers is also quite high.

6. Conclusions and future work

This paper is the first of two papers entitled "Airline Planning Benchmark Problems" that present a four step framework for generating realistic airline planning benchmark problem instances. These instances are a result of analysing rich data sets from a wide range of airlines worldwide, including all airlines in the Star and oneworld alliances. The methodology behind the

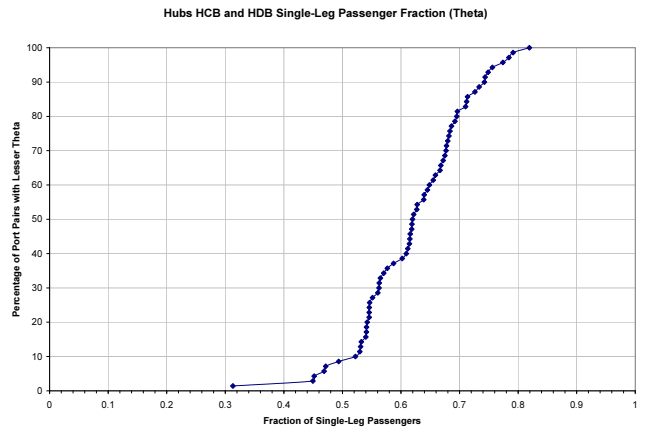
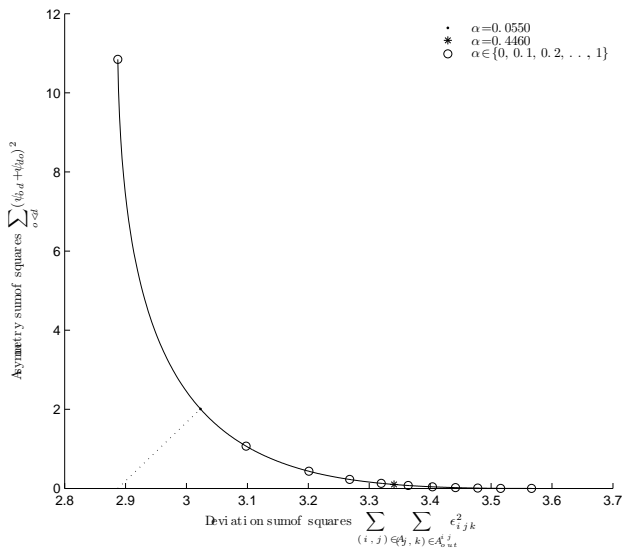


Figure 13: Frontier and single-leg passenger CDF plots for the HCB-HDB instance

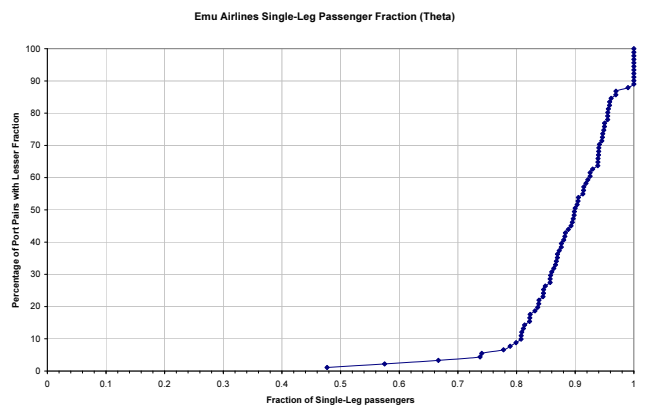
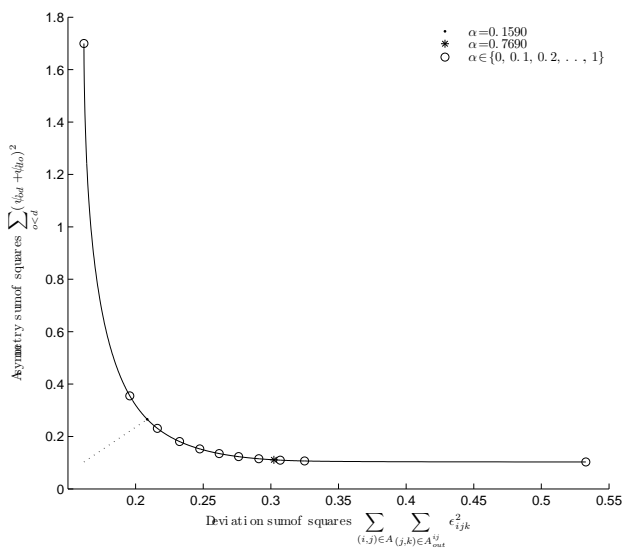


Figure 15: Frontier and single-leg passenger CDF plots for the Emu Airlines instance

first two steps in the framework, namely, characterising airline networks and OD-pair demand using limited data, were presented in this paper. The methodology of the second two steps, namely, characterising passenger groups and the allocating the OD-pair demand, is presented in the second paper (Akartunali et al., 2010a).

The thirty single-hub and three two-hub instances provide standardised data that includes OD-pair passenger demand data which is critical for the first step in the airline planning process, namely, flight schedule design. It is hoped that the availability of these instances, and a description of the methodology used to generate them, will not only make research in airline planning accessible to researchers from outside this area, but will also stimulate existing research by providing data that facilitates the accurate and repeatable comparison of the many different algorithms and techniques for the airline planning process reported in the literature.

Future work includes extending the characterisation of airline networks to include other topologies, such as linked hubs and point-to-point networks, and to generate sets of benchmarks for such networks, as well as incorporating airline resources, such as aircraft and crew, into the benchmarks.

Acknowledgements

The authors are very grateful to Ian Evans and Alan Dormer (CTI Pty Ltd) for their ongoing support and guidance on a variety of practical airline-related issues and for numerous technical suggestions and insightful feedback that improved the content and exposition of this work. This research is supported by the Australian Research Council, under Linkage Projects LP00668076 and LP0883855, and by CTI Pty Ltd.

References

- Akartunali, K., Boland, N., Evans, I., Wallace, M., Waterer, H., 2010a. Airline planning benchmark problems. Part II: Passenger groups, utility and demand allocation. Tech. rep., University of Newcastle.
- Akartunali, K., Boland, N., Evans, I., Wallace, M., Waterer, H., Smith, O., 2010b. Airline schedule design: Network design optimization and heuristics. Working paper, The University of Melbourne.
- Barnhart, C., Farahat, A., Lohatepanont, M., 2009. Airline fleet assignment with enhanced revenue modeling. *Operations Research* 57 (1), 231–244.
- Bazargan, M., 2004. *Airline Operations and Scheduling*. Ashgate Publishing Ltd.
- Coldren, G., Koppelman, F., Kasturirangan, K., Mukherjee, A., 2003. Modeling aggregate air-travel itinerary shares: logit model development at a major US airline. *Journal of Air Transport Management* 9, 361–369.
- Dumas, J., Soumis, F., 2008. Passenger flow model for airline networks. *Transportation Science* 42 (2), 197–207.
- Evans, I., 2010. Airline transit passenger percentage calculations. Tech. rep., Constraint Technologies International.
- Evans, I., Wallace, M., Waterer, H., 2010. Characteristics of airline hubs. Tech. rep., Constraint Technologies International.
- Florian, M., 1976. *Traffic Equilibrium Methods*. Springer-Verlag.
- Garrow, L., Jones, S., Parker, R., 2007. How much airline customers are willing to pay: an analysis of price sensitivity in online distribution channels. *Journal of Revenue and Pricing Management* 5, 271–290.
- Jacobs, T., Smith, B., Johnson, E., 2008. Incorporating network flow effects into the airline fleet assignment process. *Transportation Science* 42 (4), 514–529.
- Klabjan, D., 2005. Large-scale models in the airline industry. In: Desaulniers, G., Desrosiers, J., Solomon, M. M. (Eds.), *Column Generation*. Springer, pp. 163–196.

- Koppelman, F., Coldren, G., Parker, R., 2008. Schedule delay impacts on air-travel itinerary demand. *Transportation Research Part B* 42, 263–273.
- Lohatepanont, M., Barnhart, C., 2004. Airline schedule planning: Integrated models and algorithms for schedule design and fleet assignment. *Transportation Science* 38 (1), 19–32.
- Solomon, M. M., 1987. Algorithms for the vehicle routing and scheduling problems with time window constraints. *Operations Research* 35, 254–265.
- Walker, J., 2006. Time of day in airline passenger demand, presentation at the INFORMS Annual Meeting, Pittsburgh PA.
- Wojahn, O., 2002. The impact of passengers' preferences regarding time and service quality on airline network structure. *Journal of Transport Economics and Policy* 36, 139–162.
- Yan, S., Tang, C.-H., Lee, M.-C., 2007. A flight scheduling model for taiwan airlines under market competitions. *Omega* 35 (1), 61–74.
- Yan, S., Tseng, C.-H., 2002. A passenger demand model for airline flight scheduling and fleet routing. *Computers and Operations Research* 29, 1559–1581.